

INVESTIGATION OF A SUPERSONIC GAS FLOW AND HEAT TRANSFER
IN THE REGION OF AN INCIDENT SHOCK WAVE ON A CYLINDER

M.P. Teterin

N 68-30336

FACILITY FORM 602	(ACCESSION NUMBER)	(THRU)
	(PAGES)	(CODE)
	(NASA CR OR TMX OR AD NUMBER)	(CATEGORY)

Translation of "Issledovaniye Teleniya Gaza i
Teploperedachi v Oblasti Padeniya Skachka Uplotneniya
na Tsilindr, Obtekayemyy Potokom Bol'shoy
Sverkhzvukovoy Skorosti"
Izvestiya Akademii Nauk SSSR, Mekhanika
Zhidkosti i Gaza, No. 3, pp. 92-97, 1967

GPO PRICE \$ _____

CSFTI PRICE(S) \$ _____

Hard copy (HC) 3.00

Microfiche (MF) _____

ff 653 July 65



INVESTIGATION OF A SUPERSONIC GAS FLOW AND HEAT TRANSFER
IN THE REGION OF AN INCIDENT SHOCK WAVE ON A CYLINDER

M.P. Teterin

ABSTRACT. Supersonic gas flow and heat transfer in the region of an incident shock wave on a cylinder are investigated. The effect of an incident shock wave on a cylinder is reduced to the effect of a low-entropy stream formed as the result of incident-reflected shock wave interaction. Thus, the flow in the region of incidence may be considered to be a uniform low-entropy stream over a plate at certain incidence with the surrounding flow neglected. Precise measurements were made of the heat transfer on a thin walled (0.75 mm) cylinder 40 mm in diameter at $M_1 = 5$. The effect of an incident shock was observed by the erosion of material on a plexiglass cylinder visible on shadowgraph records. The effect of M on the incident shock wave effects with and without regard to the variable heat capacity ratio is investigated, and the results are given in graphs. The results confirm the existence of high intensity heat fluxes in the region where the low-entropy stream spreads over the cylinder surface.

1. It was shown in [1] that the action of an incident shock on a cylinder /92* is reduced to the action of a low entropy stream which is formed due to the interference of the incident shock wave with the shock wave reflected by the cylinder. This low entropy stream has large dynamic parameters and leads to a substantial local increase in pressure along the front surface of the cylinder. This pressure is several times greater than the pressure along the critical line of the cylinder in the unperturbed flow. We should expect intense velocity gradients at the place where this stream spreads over the front surface of the cylinder when the width of this two-dimensional supersonic stream is small (from 3 to 5% of the cylinder diameter). These intense velocity gradients substantially exceed the velocity gradients along the critical line of a cylinder in an unperturbed flow.

The simultaneous combination of increased pressure and velocity gradients at the critical point C where the low entropy streams spread out enables us to consider this point as the place where we have a maximum heat transfer on the frontal surface.

As in the case of the total pressure computation, the stream method can be used for the approximate computation of heat transfer at the critical point C of the cylinder. The basic parameters of a low-entropy stream were determined in front of the critical point in [1].

* Numbers in the margin indicate pagination in the foreign text.

Then the flow in the region of the incident shock on the cylinder may be regarded as the flow of a two-dimensional uniform low-entropy stream over a plate at some angle α , disregarding the surrounding flow (Figure 1).

The symbols used in Figure 1 correspond to symbols adopted in [1].

Thus [2] we shall assume that the stream line of the supersonic low-entropy stream at the critical point C passes through the normal shock wave 7. It is necessary to know the velocity gradient at point C as well as the parameters of the incident stream to determine the heat transfer at this point (point C is the projection of critical line C - the line over which the low-entropy stream spreads out and which is perpendicular to the critical generatrix of the cylinder). It is necessary to know the gradient of increase of the incident stream at this point as well as its parameters. We take the value of the velocity gradient computed in [3] for a two-dimensional stream of an incompressible fluid as the lower limit of possible values of the velocity gradient:

$$du/dx = \sqrt{1/2} \pi u / H \sin^2 \alpha \quad (1.1)$$

In the above equation u is the velocity along the separating stream line behind shock 7 and x is the distance measured along line EF (Figure 1). If we substitute the velocity gradient (1.1) into the equation for the dimensionless heat transfer parameter given by the Stanton number S_∞ along the critical line of the cylinder in the case of a laminar boundary layer [5], we obtain.

$$S_\infty(C) = \frac{0.505}{\sin \alpha} \left(\frac{\rho_0 u_0}{\rho_1 u_1} \right)^{1/2} \left(\frac{\mu_0}{\mu_1} \right)^{1/2} \left(\frac{\rho_0}{\rho_1} \right)^{1/2} \left(\frac{\mu}{\rho_1 u_1 H} \right)^{1/2} P^{-0.6} \quad (1.2)$$

which can be used to compute the heat transfer at the critical point of a two-dimensional supersonic stream with width H incident at an angle α on a plate. In the above equation ρ_0 and μ are density and viscosity at critical point C while P is the Prandtl number. The numerical subscripts correspond to the superscripts for the shock waves in the interference region [1] and show that the particular quantity is determined in the flow region behind the specified shock. The upper limit for the value of the velocity gradient at the critical point of the spreading stream may be assumed to be equal to the velocity gradient obtained by generalizing the results of [5].

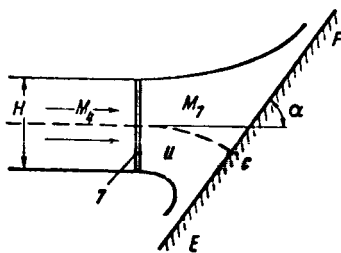


Figure 1.

The true values of the velocity gradient lie between these two limits and apparently are closer to the upper limit. The width of the "path" where the true values of the gradient are unknown increases with M . The maximum width in our computations occurs when $M_4 = 2.7$, which corresponds to $M_1 = 25$ and to a value of $S_\infty(C) = 27\%$. When $M_1 = 5$ the width of this path is equal to 11%. The calculation of the dimensionless heat transfer

parameter $S_{\infty}(C)$ when determining the velocity gradient from the upper limit is carried out with the aid of equation

$$S_{\infty}(C) = \frac{0.505}{\gamma \lambda_4} \left(\frac{\rho_4 u_4}{\rho_1 u_1} \right)^{1/2} \left(\frac{\rho_0}{\rho_1} \right)^{1/2} \left(\frac{\mu_0}{\mu_1} \right)^{1/2} \left(\frac{\mu_1}{\rho_1 u_1 H} \right) \frac{P_{-0.8}}{\sin \alpha} \quad (1.3)$$

In the above equation λ_4 is the ratio of the low-entropy stream to the critical velocity of sound in the stream. When the heat transfer at critical point C is computed with the aid of (1.2), and (1.3) it is also necessary to know the width of the low-entropy stream H. Unfortunately, at the present time, it is not possible to determine the separation distance of the shock wave from the cylinder (and consequently the width of the low-entropy stream) without an exact solution of gas dynamics equations for the entire region where the two shock waves interact. However the width of the stream can be determined semiempirically if the distance AB between the junction points of the λ -shock is known. This is done by means of equation

$$H = AB \frac{\sin(\theta_3 - \delta_3) \sin(\theta_4 - \delta_4)}{\sin \theta_4} \quad (1.4)$$

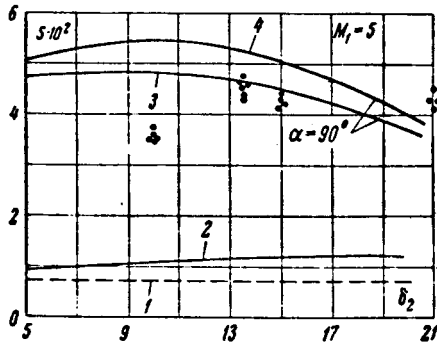


Figure 2.

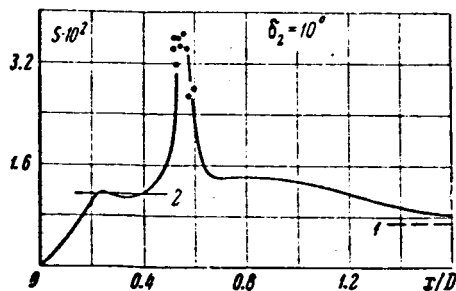


Figure 3.

In the above equation θ_i is the slope of the i -th shock wave while δ_i is the flow rotation angle in this shock. The quantity AB is obtained experimentally at $M_1 = 5$ as a function of the incident shock wave intensity. This experimentally determined relationship was used to compute the numbers $S_{\infty}(C)$ on the M20 electronic digital computer using the same value $M_1 = 5$. The numbers

$S_{\infty}(C)$ were computed both for the upper and lower limits of pressure gradient variation. The results of the calculations for $M_1 = 5$ are shown in Figure 2 in the form of two curves. The curve computed by means of equation (1.2) is designated by the numeral 3 while the curve computed by means of equation (1.3) is designated by 4. The curves are functions of the incident shock wave intensity measured by the flow rotation angle δ_2 in the incident shock. The rela-

tionship $S_{\infty} = S_{\infty}(C, \delta_2)$, like the relationship for the total pressure \bar{p}_{07} [1], /94 has a maximum value with respect to δ_2 but this maximum is less pronounced than the pressure maximum when $M_1 = 5$. It was assumed in the calculations that the angle between the stream direction and the frontal generatrix of the cylinder was 90° because the relation $\alpha = \alpha(\delta_2)$ was not known.

The heat transfer of a thin-walled steel cylinder was carefully measured in order to check the results of the calculations. The wall thickness of the cylinder was 0.75 mm and its external diameter was 40 mm. The cylinder was tested in the TsAGI wind tunnel at $M_1 = 5$. The results of the heat transfer measurements were processed on the electronic digital computer using a special program for processing data from heat experiments. As an illustration Figure 3 shows the results of the comprehensive measurement of heat transfer at $M_1 = 5$ and $\delta_2 = 10$ in the form of the relation $S^\infty = S^\infty(x/D)$ along the critical generatrix of the cylinder. This relationship shows that there is a "peak" in the distribution of heat transfer. Heat transfer at the point where the low-entropy stream spreads is approximately 5 times greater than the heat transfer of a cylinder in an unperturbed flow [4]. The distribution of S^∞ over x/D shows that heat transfer in the vicinity of the "peak" is approximately two times greater than the theoretical value designated by numeral 1 for the cylinder [4] and decreases in the direction of large values of x/D almost to the theoretical value. We should also mention that there is good agreement between experiment and theory. The theoretical values are designated by the numeral 2 in Figure 3 [6] in the region of the flow which has passed shocks 2 and 6 [1].

A comparison of the computed relation $S^\infty = S^\infty(C, \delta_2)$ with the experimental peak values of heat transfer in the region where the low-entropy stream spreads, is shown in Figure 2. As in the case of pressure [1] there is good agreement between computed peak values of heat transfer and experimental values in the range of large incident shock wave intensities $\delta_2 > 17^\circ$. For lower intensities ($\delta_2 = 10^\circ$) the experimental values are below the theoretical values for same reasons, i.e. due to the effect of viscosity on the erosion of the low-entropy stream. For comparison Figure 2 shows the values of the heat transfer along the critical lines corresponding to a cylinder (curve 1) in an unperturbed flow [4] and the values of heat transfer (curve 2) computed by means of equations in [6] on a cylinder in the region of flow behind shocks 2 and 6 [1]. These are several times less than the heat transfer in the region where the low-entropy stream spreads out.

Along with measurements of heat transfer, the intense thermal action in the region of the shock drop was observed directly in an experiment on the erosion of material, using a plexiglas model of the cylinder (with a diameter of 40 mm). Figure 4 shows the Schlieren photographs of the model at three successive moments of time. The regions of maximum heat transfer are clearly seen at the place where the low-entropy stream spreads and at the place where the boundary layer, broken off the wedge, is attached. Thus the results of investigations on heat transfer in the region of shock wave incident on a cylinder, together with the results earlier published concerning the intense action of the incident shock [1], show that there are strong thermal fluxes at the place where the low entropy stream spreads.

2. The effect of the incident flow Mach number M on the mechanical [1] and/95 thermal action of the shock wave incident on the cylinder is illustrated in

Figures 5 and 6. In these figures the ratio of the total pressure in the stream \bar{p}_{07} to the pressure at the critical line of the cylinder in an unperturbed flow ($\bar{p}_{07} = 1.81$) (Figure 5) and the relation $S = S_{\infty}(C)/S_{\infty}$ (Figure 6) of the heat transfer at critical point C to the heat transfer S_{∞} on the critical line of the cylinder [4] are presented for critical point C where the low-entropy stream spreads out, as a function of incident shock wave intensity.

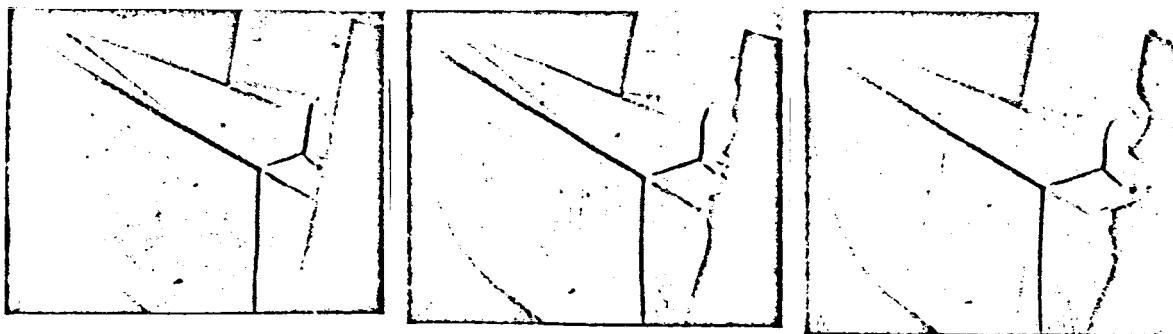


Figure 4.

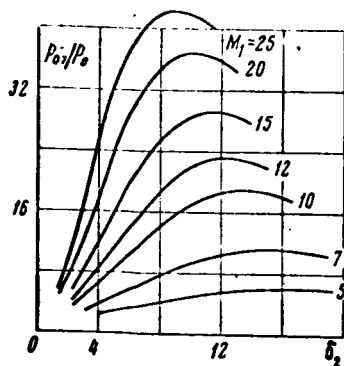


Figure 5.

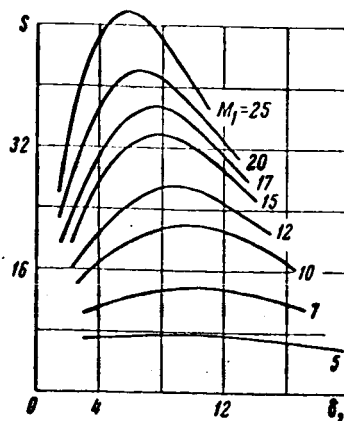


Figure 6.

The data of Figures 5 and 6 show that there is a very strong increase in pressure and heat transfer at the critical point C when M increases.

The computations were carried out on the M-20 electronic digital computer using equations presented in [1] for the ratio of total pressures and using equations (1.2), (1.3) of our work for the ratio of $S_{\infty}(C)$ numbers, assuming that the gas remains ideal at high Mach numbers. Also the data of [7 and 8] were used during the calculation of heat transfer to extrapolate the experimental relationship $H = H(\delta_2)$ to large values of M .

3. Under actual conditions when the Mach numbers M are high the deceleration of the gas in the shock wave or in a system of shock waves leads to a substantial increase in its temperature, which is accompanied by dissociation and ionization of gas molecules as well as by associated relaxation processes. As a result, the exact solution of the problem of shock wave interference, taking into account changes in the thermodynamic properties of the gas, becomes a complex problem. However it is of interest to estimate the nature of the mechanical and thermal action of the incident shock wave taking into account variations in

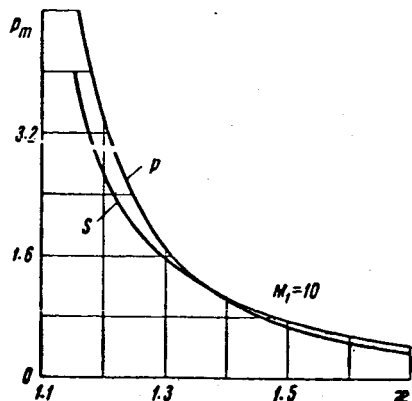


Figure 7.

the ratio of specific heats κ . It is well known that κ decreases as the velocity of the incident flow increases.

Figure 7 shows the computed values of the dimensionless pressure coefficients $\bar{p}_{07\max} = p(\kappa)$ which are maximum with respect to δ_2 , for $M_t = 10$ expressed as the relation

$$p_m = \bar{p}_{07\max}(\kappa) / \bar{p}_{07\max} |_{\kappa=1.4}$$

and the heat transfer coefficients $S_{\infty\max}(C) = S(\kappa)$ as the relation

$$S_m = S_{\infty\max}(C, \kappa) / S_{\infty\max}(C) |_{\kappa=1.4}$$

It is difficult to take into account the effect of κ on heat transfer at the critical point where the low-entropy stream spreads because there are no data on the velocity gradient at point C (Figure 1) and on the separation of the shock wave as a function of κ . Therefore the curve $S_{\infty}(C)$ shows changes in heat conductivity due only to the variation in the dynamic parameter of the stream, such as M , p , and ρ .

The curves in Figure 7 show that in an actual case of flow past a cylinder at high Mach numbers the mechanical and thermal reaction of the incident shock wave will be more intense than those in the case of an ideal gas.

4. The presence of a breakaway region in front of the cylinder installed on a plate across the incident flow also leads to the formation of a low-entropy stream which produces an intense mechanical [1] and thermal reaction. Measurements of heat transfer on a cylinder of this type (diameter of 50 mm) were carried out back in 1964 at $M_1 = 5$ but the detailed results of these investigations are not presented in this article. Figure 2 shows the experimental values of $S_{\infty}(C)$ obtained in the experiment corresponding to the critical point C when $\delta_2 = 13^\circ.5$. These values are in good agreement with experimental values obtained at a later time (see Section 1).

5. The sweep-back angle of the cylinder has a very interesting effect on the flow picture as well as on the mechanical and thermal reactions of the low-entropy stream on the cylinder. As the sweep-back angle of the cylinder is increased from a zero value (see Figure 8, a¹) the intensity of the detached bow wave of the cylinder decreases, this produces a change in the pressure field of the subsonic region (behind shocks 5 and 6 in Figure 2, [1] surrounding the low-entropy stream. As the sweep-back angle is increased further this change in the pressure field causes the junction points of the λ -shocks to

¹The flow picture in Figure 8 was obtained for $M_1 = 5$ and $\delta_2 = 15^\circ$.

converge (Figure 8, b) and when $\chi = 30^\circ$ (Figure 8, c) these points practically run together into a single point.

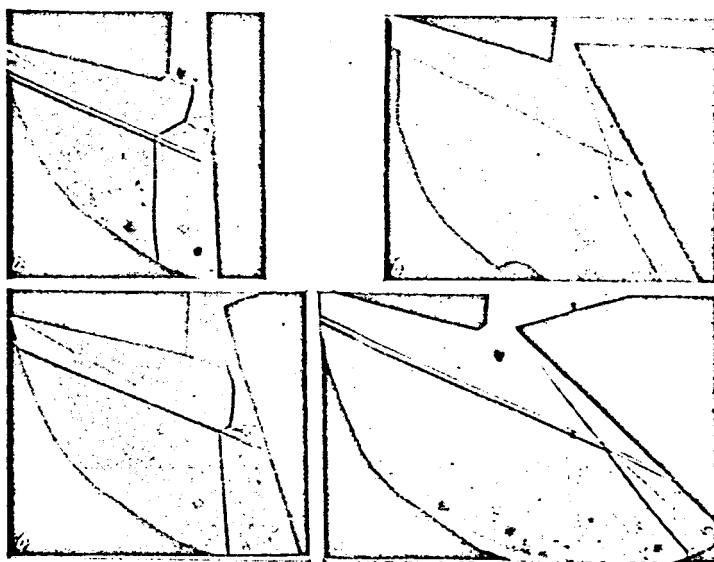


Figure 8.

According to the Wuest-Wecken diagram [9, 10] an increase in the sweep angle, which leads to a decrease in the angle of the resulting shock, indicates that the boundary AD_1 of region G_1 is approached (the symbols are defined in [9]). This boundary is noteworthy because when $\kappa = 1.4$, the Mach number behind the resulting shock is close to 1. A further increase in the sweep-back angle leads to region G_2 which determines the region where λ -shocks exist (with two incident and one reflected shocks).

It turns out that the considered flow scheme with two successive λ -shocks disappears completely (Figure 8, d), and the angular points of the λ -shocks blend into one, thereby forming a λ -shock which belongs to region G_2 . Thus, when a system consisting of two λ -shocks disappears the low-entropy stream produced by this system also disappears, together with all of the reactions produced by this stream.

The above information can be used to obtain the approximate limits for the maximum sweep-back angles (the maximum sweep-back angles $\chi = 44^\circ, 38^\circ, 35^\circ.5, 35^\circ, 34^\circ.6, 34^\circ.5$ correspond to the numbers $M_1 = 3, 5, 10, 15, 20$ and 25) beyond which the system of shocks which produces the low-entropy stream, as a function of M_1 of the incident flow, disappears. The results on the maximum sweep-back angle were compared with experimental results obtained at $M_1 = 5$, a sweep-back angle of approximately 38° and an incident shock flow rotation angle of $\delta_2 = 15^\circ$ for three angles of sweep-back, $\chi = 0, 30$ and 45° . The

/97

experimental data are rather convincing evidence of the disappearance of the peak in the distribution of pressure and heat transfer when the sweep-back angle lies beyond the boundary of the maximum angles. If both the pressure and the heat conductivity have a sharp maximum when $\chi = 0$ and 30° , then when $\chi = 45^\circ$ they are practically constant, i.e. they do not have extreme values.

Thus the results of the experiment confirm the validity of conclusions reached concerning the disappearance of the system of shocks which generates the low-entropy stream when the sweep-back angle of the cylinder is increased and hence the disappearance of mechanical and thermal reactions of this stream on the cylinder.

REFERENCES

1. Teterin, M.P.: Investigation of gas flow in the region of the shock wave incident on a cylinder in a supersonic flow [Issledovaniye techeniya gaza v oblasti padeniya skachka uplotneniya na tsilindr, obteyemyy potokom sverkhzvukovoy skorosti.] Izv. AN SSSR, MZhG, No. 2, 1967.
2. Neylapd, V.Ya. and G.I. Taganov: On heat transfer to a body near the frontal breakaway zone at hypersonic flow velocities Inzh. Zh., No. 3, 1961.
3. Schach, W.: Ingr. Arch., Vol. 5, pp. 245-265, 1934.
4. Driest, E.: The problem of Aerodynamic Heating, Aeronaut. Engng. Rev., Vol. 15, No. 10, 1965.
5. Bazzhin, A.P.: On the computation of supersonic gas flow past a plane plate with an attached shock. Inzh. Zh., Vol. 3, No. 2, 1963.
6. Beckwith, I.E.: Similar Solutions for the Compressible Boundary Layer on a Jawed Cylinder with Transpiration Cooling, NACA TN 4345, 1958.
7. Belotserkovskiy, O.M.: The computation of the flow past a circular cylinder with a detached shock wave, Vychisl. Matem., No. 3, 1958.
8. Belotserkovskiy, O.M.: The computation of flow past axisymmetric bodies with a detached shock wave by means of an electronic computer, PMM, Vol. 24, No. 3, 1960.
9. Wuest, W.: On the theory of Y-shaped shock waves. Collected works "Gas Dynamics". "Gazovaya dinamika" [Gas Dynamics], Foreign Literature Press, 1950.
10. Wecken, F.: The limiting positions of Y-shaped shock waves. Mekhanika [Mechanics] collection of translations and surveys of foreign periodic literature. No. 4, 1950.

Translated for the National Aeronautics and Space Administration under Contract No. NASw-1695 by Techtran Corporation, P.O. Box 729, Glen Burnie, Md. 21061